ORGANIC LETTERS

XXXX
Vol. XX, No. XX
000–000

What Controls Regiochemistry in 1,3-Dipolar Cycloadditions of Münchnones with Nitrostyrenes?

Justin M. Lopchuk, Russell P. Hughes,* and Gordon W. Gribble*

Department of Chemistry, Dartmouth College, Hanover, New Hampshire 03755, United States

gordon.w.gribble@dartmouth.edu; Russell.P.Hughes@dartmouth.edu

Received August 20, 2013

ABSTRACT

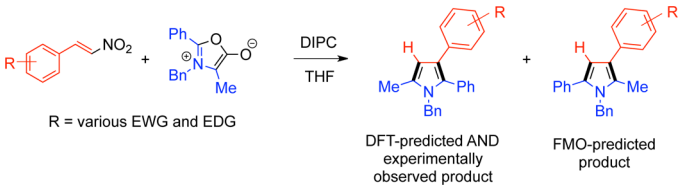

The distinct experimentally observed regiochemistries of the reactions between mesoionic münchnones and β-nitrostyrenes or phenylacetylene are shown by DFT/BDA/ETS-NOCV analyses of the transition states to be dominated by steric and reactant reorganization factors, rather than the orbital overlap considerations predicted by Frontier Molecular Orbital (FMO) Theory.

Münchnones (1,3-oxazolium-5-olates)[1] are five-membered mesoionic heterocycles that undergo 1,3-dipolar cycloadditions with acetylenes and electron-deficient alkenes.[2] Although the reaction of münchnones with acetylenic dipolarophiles[3] has been studied for many years, more recent investigations utilize nitroalkenes as synthetic equivalents of alkynes.[4] A striking regiochemical feature of these reactions is the lack of correlation with FMO theory,[1−5] in contrast to its utility in predicting the outcome of many other cycloadditions.[2]

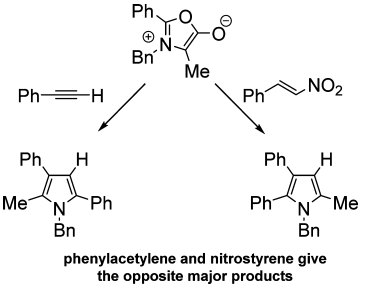

Figure 1. Experimentally observed products from 1,3-dipolar cycloadditions of münchnones and dipolarophiles.

Although some DFT calculations have been reported to rationalize the experimentally observed regiochemistry,[3a,4c] the specific factors involved remain elusive, but are assumed to comprise a combination of electronic, steric, and stereoelectronic effects. Herein we report a combination of synthetic and computational studies that shed light on the factors contributing to the regioselectivity observed in these reactions.

During investigations[5] into the reaction of nitroindoles, nitrovinylindoles, and nitrovinylpyridines with münchnones, we became interested in the general reactivity and

(1) Gribble, G. W. Mesoionic Oxazoles. In *The Chemistry of Heterocyclic Compounds, Oxazoles: Synthesis, Reactions, and Spectroscopy*; Taylor, E. C., Wipf, P., Eds.; John Wiley & Sons: Hoboken, NJ, 2003; Vol. 60, Part A, p 473.

(2) Gribble, G. W. Mesoionic Ring Systems. In *The Chemistry of Heterocyclic Compounds: Synthetic Applications of 1,3-Dipolar Cycloaddition Chemistry Toward Heterocycles and Natural Products*; Padwa, A., Pearson, W. H., Eds.; John Wiley & Sons: Hoboken, NJ, 2002; Vol. 59, p 681.

(3) (a) Padwa, A.; Burgess, E. M.; Gingrich, H. L.; Roush, D. M. *J. Org. Chem.* **1982**, *47*, 786. (b) Coppola, B. P.; Noe, M. C.; Schwartz, D. J.; Abdon, R. L.; Trost, B. M. *Tetrahedron* **1994**, *50*, 93. (c) St-Cyr, D. J.; Morin, M. S. T.; Belanger-Gariepy, F.; Arndtsen, B. A.; Krenske, E. H.; Houk, K. N. *J. Org. Chem.* **2010**, *75*, 4261.

(4) (a) Avalos, M.; Babiano, R.; Bautista, I.; Fernandez, J. I.; Jimenez, J. L.; Palacios, J. C.; Plumet, J.; Rebolledo, F. *Carbohydr. Res.* **1989**, *186*, C7. (b) Nesi, R.; Giomi, D.; Turchi, S.; Tedeschi, P.; Ponticelli, F. *Gazz. Chim. Ital.* **1993**, *123*, 633. (c) Avalos, M.; Babiano, R.; Cabanillas, A.; Cintas, P.; Jimenez, J. L.; Palacios, J. C. J. *Org. Chem.* **1996**, *61*, 7291. (d) Gribble, G. W.; Pelkey, E. T.; Switzer, F. L. *Synlett* **1998**, 1061.

(5) (a) Gribble, G. W.; Pelkey, E. T.; Simon, W. M.; Trujillo, H. A. *Tetrahedron* **2000**, *56*, 10133. (b) Lopchuk, J. M.; Gribble, G. W. *Heterocycles* **2011**, *82*, 1617. (c) Lopchuk, J. M.; Gribble, G. W. *Tetrahedron Lett.* **2011**, *52*, 4106.

10.1021/ol402385v

regioselectivity of β-nitrostyrene derivatives as the dipolarophiles in these 1,3-dipolar cycloadditions (Figure 1).

The nitroalkenes (**1**–**13**, Table 1) utilized in this work were prepared by condensation of the appropriate benzaldehyde derivatives with nitromethane (Henry reaction).[6] Most of these reactions proceed in excellent yield (see Supporting Information (SI)), although two strong electron-withdrawing groups (NO_2 and CF_3) are notable exceptions.

We used a standard method[5] to synthesize unsymmetrical münchnones **16** and **17** from the appropriate ethyl bromoester in high yield (see SI for details). The münchnones were not isolated, but instead generated *in situ* by cyclodehydration with *N*,*N*′-diisopropylcarbodiimide (DIPC) (Scheme 1). Thus, a mixture of the münchnone precursors, **14** and **15**, and the nitroalkenes in THF was treated with DIPC, and the mixture was heated to reflux for 12–36 h to yield the desired substituted pyrroles as mixtures of two isomers (Table 1). The indicated regiochemistry of the products was confirmed by 1D NOESY (irradiation of the pyrrole ring proton) and the presence (or absence) of long-range coupling between the ring proton and the methyl group.

Scheme 1. Cyclization of Unsymmetrical Münchnones

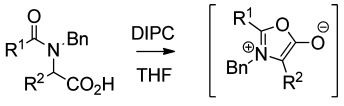

14: $R^1 = CH_3$; R^2 = Ph **16**: $R^1 = CH_3$; R^2 = Ph
15: R^1 = Ph; $R^2 = CH_3$ **17**: R^1 = Ph; $R^2 = CH_3$

These results demonstrate that the reactions are quite insensitive to varying electron-donating or -withdrawing substituents on the phenyl ring of the nitroalkene, resulting in minimal effects on product yields and isomer distributions. However, when the steric bulk of the phenyl ring on the nitroalkene is significantly increased (e.g., dual ortho substitution; entries 12, 13) yields decrease dramatically but product ratios are altered only slightly (unreacted starting material comprises the bulk of the reaction mixture).

Münchnone **17** proved higher yielding in every case and was more regioselective with all but the most sterically hindered nitroalkenes (mesityl **12** and anthracene **13**). Competition experiments also indicate that **17** was more reactive than münchnone **16** (see SI for details).

Density Functional Theory (DFT) calculations were carried out at the B3LYP-D3/6-311G**++ level,[7,8] as implemented in the Jaguar[9] suite of programs. Full details are provided as SI. Examination of the Kohn–Sham HOMO/LUMO energies for each set of nitrostyrene and münchnone starting materials showed a significantly better energy match between the münchnone HOMO and the nitrostyrene LUMO, rather than vice versa.[11] As observed previously using FMO theory,[12] the DFT HOMO/LUMO coefficients do not predict the correct regiochemistry for cycloaddition. Similar observations hold for the reactions of both münchnones with phenylacetylene. Transition states corresponding to the eight regio- and stereochemical options for nitrostyrene/münchnone cycloadditions were located, as were those for the four regiochemical options for phenylacetylene/münchnone cycloaddition; each was confirmed to be the correct transition state by observation of a single imaginary frequency and by subsequent intrinsic reaction coordinate (IRC) calculations. These computations are excellent predictors for the regiochemical selectivity for each münchnone and even correctly predict the reversal of regiochemistry observed in entry 6. In all cases the cycloaddition proceeds in a single step via an unsymmetrical transition state in which one C–C bond is more completely formed than the other; initial cycloaddition is the slow step, and loss of CO_2 to give the pyrrole product(s) is fast. For example, the lowest energy transition state

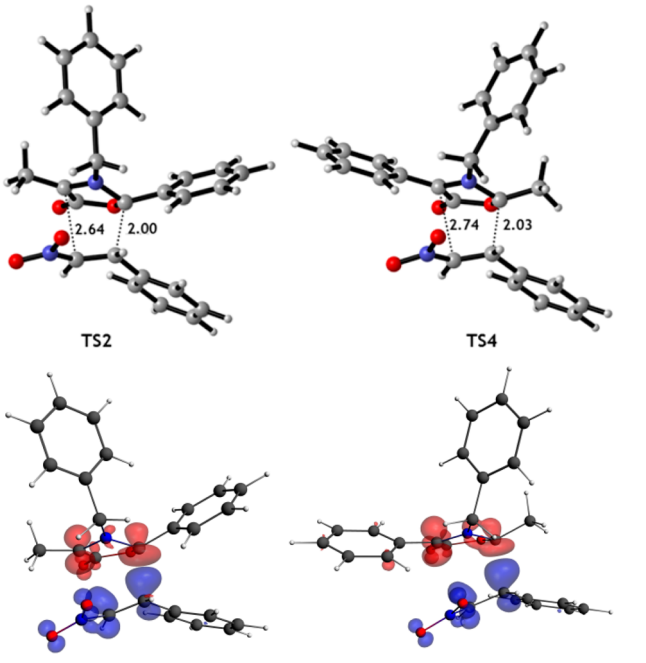

Figure 2. (Top) Lowest energy transition states for reaction of **17** (TS2) and **16** (TS4) with nitrostyrene, with C–C distances (Å). (Bottom) Principal deformation densities in the same transition states (0.005e isosurfaces), showing electron "flow" from red to blue between reactants.

(6) Cote, A.; Lindsay, V. N. G.; Charette, A. B. *Org. Lett.* **2007**, *9*, 85.
(7) (a) Lee, C.; Yang, W.; Parr, R. G. *Phys. Rev. B* **1988**, *37*, 785–789. (b) Becke, A. D. *J. Chem. Phys.* **1993**, *98*, 5648–5652. (c) Becke, A. D. *J. Chem. Phys.* **1993**, *98*, 1372–1377.
(8) (a) Dunning, T. H.; Hay, P. J. In *Modern Theoretical Chemistry, Vol. 4: Applications of Electronic Structure Theory*; Schaefer, H. F., III, Ed.; Plenum, NY: 1977. (b) Hay, P. J.; Wadt, W. R. *J. Chem. Phys.* **1985**, *82*, 270–283. (c) Hay, P. J.; Wadt, W. R. *J. Chem. Phys.* **1985**, *82*, 299–310. (d) Wadt, W. R.; Hay, P. J. *J. Chem. Phys.* **1985**, *82*, 284–298.
(9) *Jaguar*, versions 7.0–7.7; Schrödinger, LLC: New York, NY, 2007–2010.
(10) (a) Glendening, E. D.; Badenhoop, J. K.; Reed, A. K.; Carpenter, J. E.; Bohmann, J. A.; Morales, C. M.; Weinhold, F. *NBO 5.0*, Theoretical Chemistry Institute, University of Wisconsin; Madison: 2001. (b) Weinhold, F.; Landis, C. R. *Valency and Bonding: A Natural Bond Orbital Donor-Acceptor Perspective*; Cambridge University Press: Cambridge, 2005.

Table 1. Results of Münchnone Cyclizations

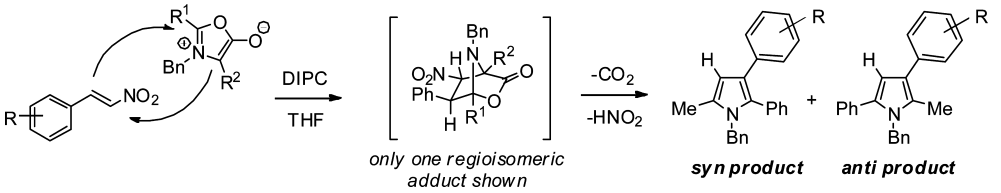

		reaction with münchnone **17**			reaction with münchnone **16**		
entry	R	products	ratio (syn:anti)[a]	yield (%)[b]	products	ratio (syn:anti)[a]	yield (%)[b]
1	H (**1**)	**18a:18b**	92:8	94	**18a:18b**	14:86	81
2	4-Cl (**2**)	**19a:19b**	95:5	80	**19a:19b**	24:76	71
3	3-F (**3**)	**20a:20b**	88:12	97	**20a:20b**	19:81	75
4	4-NMe_2 (**4**)	**21b:21b**	81:19	52	**21b:21b**	17:83	45
5	4-OMe (**5**)	**22a:22b**	94:6	65	**22a:22b**	20:80	62
6	4-NO_2 (**6**)	**23a:23b**	85:15	58	**23a:23b**	57:43	50
7	4-Me (**7**)	**24a:24b**	89:11	64	**24a:24b**	14:86	63
8	4-CF_3 (**8**)	**25a:25b**	92:8	70	**25a:25b**	26:74	67
9	4-Ph (**9**)	**26a:26b**	91:9	61	**26a:26b**	22:78	57
10	2-NO_2 (**10**)	**27a:27b**	95:5	86	**27a:27b**	26:74	67
11	2-Me (**11**)	**28a:28b**	89:11	76	**28a:28b**	34:66	68
12	2,4,6-Me (**12**)	**29a:29b**	62:34	12	**29a:29b**	11:89	7
13	anthracen-9-yl (**13**)	**30a:30b**	75:25	18	**30a:30b**	17:83	8
14	phenylacetylene	**18a:18b**	1:>99	83	**18a:18b**	>99:1	32

[a] Product ratios were determined by NMR integration; regiochemistry was determined by NOE resonance of the pyrrole ring proton. [b] Yields refer to isolated products after column chromatography.

(TS2; $\Delta G^{\ddagger}$ = 13.0 kcal/mol) for reaction of **17** with nitrostyrene to give the syn product and that for reaction of **16** (TS4; $\Delta G^{\ddagger}$ = 14.2 kcal/mol) to give the anti product are illustrated in Figure 2. Details for all transition states are provided as SI.

For syn-selective reaction of **17** TS2 is 2.6 kcal/mol more favored than the lowest energy transition state leading to the anti product, while for antiselective **16** TS4 lies 1.9 kcal/mol lower than that favoring the syn product. This is consistent with the observed higher selectivities seen for münchnone **17** (Table 1). All transition states with the NO_2 group directed toward the lactone are more significantly disfavored. Table 2 summarizes DFT predictions and experimental outcomes. It is noteworthy that use of the B3LYP functional without the Grimme (D3) dispersion correction resulted in considerably higher activation barriers (see SI) for these associative reactions, emphasizing the importance of including dispersion interactions between the two reacting fragments.[13] In order to examine further the nature of the transition states, each was subjected to a fragment energy decomposition analysis (EDA/B3LYP-D3/TZ2P), based on the Extended Transition State (ETS) method,[14] as implemented in the ADF computational package.[15] The ETS approach partitions the total energy of interaction (E_{int}, corresponding to the activation energy) between reacting fragments at the transition state into the energy costs to deform the reagent fragments into their transition state geometries (E_{prep}) and Pauli repulsion between fragments (E_{Pauli}) as well as the energy stabilization resulting from attractive electrostatic interaction (E_{estat}) and covalent interactions (E_{orb}).

Table 2. Summary of Experimental Observations vs Predictive Methods

	observed		prediction			
			FMO		DFT	
münchnone	**17**	**16**	**17**	**16**	**17**	**16**
phenylacetylene	anti	syn	syn	anti	anti	syn
β-nitrostyrene	syn	anti	anti	syn	syn	anti

The use of this kind of method for analysis of energy components in transition states has led to the activation–strain[16] and distortion–interaction[17] models. Furthermore,

(11) For example: β-Nitrostyrene (HOMO −7.323 eV; LUMO −3.097 eV): Münchnone **17** (HOMO −5.032 eV; LUMO −1.866 eV). Full details are provided in the SI.

(12) Gribble, G. W.; Trujillo, H. A., unpublished results.

(13) (a) Goerigk, L.; Grimme, S. *Phys. Chem. Chem. Phys.* **2011**, *13*, 6670–6688. (b) Grimme, S.; Antony, J.; Ehrlich, S.; Krieg, H. *J. Chem. Phys.* **2010**, *132*, 154104.

(14) (a) Ziegler, T.; Rauk, A. *Inorg. Chem.* **1979**, *18*, 1558–1565. (b) Ziegler, T.; Rauk, A. *Inorg. Chem.* **1979**, *18*, 1755–1759.

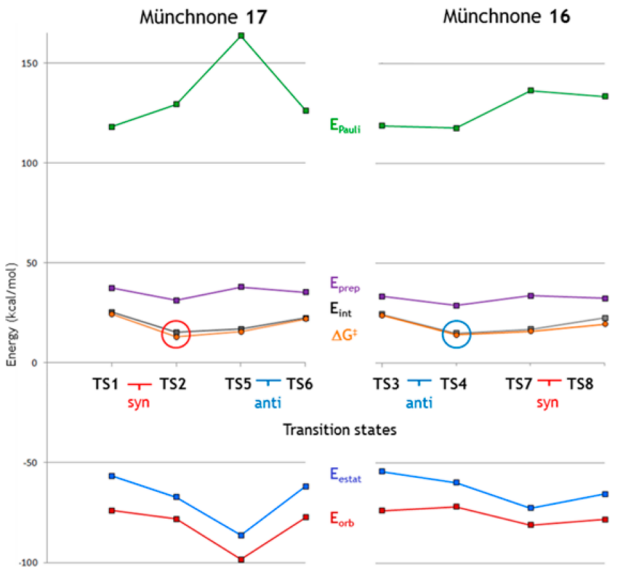

Figure 3. Energy components from energy decomposition analyses of each set of transition states for reactions of **17** and **16** with nitrostyrene.

the recently established extension of the ETS method to the evaluation of Natural Orbitals for Chemical Valence (NOCV)[18] allowed the overall orbital contribution E_{orb} to be further partitioned into component contributions. Figure 2 also shows an electron deformation density plot of the principal NOCV component (~75% of the total E_{orb}) illustrating how electron density is redistributed between fragments in the lowest energy transition states for each system. It is clear that the major contributor involves donation from münchnone to styrene, as expected from HOMO/LUMO energy considerations. A more complete picture emerges from Figure 3, which shows plots of the energy components for the transition states for reactions of **17** and **16** with nitrostyrene. It is important to note that the values of E_{int} derived by this method using the Slater type TZ2P basis functions implemented in ADF closely match the values of $\Delta G^{\ddagger}$ obtained using the Gaussian type 6-311G basis functions of Jaguar, and likewise predict the lowest energy transition states TS2 and TS4. For **17**, the most attractive bonding interactions E_{estat} and E_{orb} favor TS5, leading to the anti product, consistent with FMO predictions.

However TS5 also has both the highest Pauli repulsions and energetic cost of distortion of the reactants, driving it above TS2, and leading to the observed selectivity. Similar arguments pertain for reactions of **16** with nitrostyrene (Figure 3) and for reactions of phenylacetylene with both münchnones (see SI). Similar differences between FMO and DFT predictions in addition reactions of linear 1,3-dipoles with alkenes and alkynes have been reported by Ess and Houk as resulting from distortion effects overwhelming FMO control.[18]

As noted above these cycloadditions appear to have a strong steric component. A single ortho substituent on the phenyl ring of the nitrostyrene (entries 10, 11) is well tolerated; the transition state likely has a degree of flexibility when forming the initial bond. However, incorporation of two ortho substituents with either sp^2 or sp^3 carbons (entries 13 and 12, respectively) significantly attenuates the reactivity. Presumably initial bond formation occurs next to the now sterically congested mesityl and anthracenyl rings and thus proceeds sluggishly. In addition to the low yields, the otherwise minor regioisomer comprises a higher percentage of the product mixture. These lower selectivities are also correctly predicted by DFT.

In summary, the 1,3-dipolar cycloaddition between münchnones and β-nitrostyrenes provides a convenient synthesis of substituted pyrroles, in a reaction with regioselectivity that seems to be governed by steric and reactant reorganizational factors rather than FMO overlap. Further synthetic and computational investigations into the electronic and steric parameters of these types of reactions are underway and will be reported in due course.

Acknowledgment. R.P.H. acknowledges the National Science Foundation for operating grant funds that helped purchase some computational resources at Dartmouth. J. M.L. acknowledges a GAANN Fellowship from the U.S. Department of Education. G.W.G. acknowledges support by the Donors of the Petroleum Research Fund (PRF), administered by the American Chemical Society, and support by Wyeth.

Supporting Information Available. Experimental procedures, computational methods and data, and spectroscopic data. This material is available free of charge via the Internet at http://pubs.acs.org.

The authors declare no competing financial interest.

(15) (a) *ADF 2010–2012*; SCM, Theoretical Chemistry, Vrije Universiteit, Amsterdam, The Netherlands, http://www.scm.com. (b) Guerra, C. F.; Snijders, J. G.; Velde, G. t.; Baerends, E. J. *Theor. Chem. Acc.* **1998**, *99*, 391–403. (c) te Velde, G.; Bickelhaupt, F. M.; Baerends, E. J.; Fonseca Guerra, C.; van Gisbergen, S. J. A.; Snijders, J. G.; Ziegler, T. *J. Comput. Chem.* **2001**, *22*, 931–967.

(16) van Zeist, W.-J.; Bickelhaupt, F. M. *Org. Biomol. Chem.* **2010**, *8*, 3118–3127.

(17) Ess, D. H.; Houk, K. N. *J. Am. Chem. Soc.* **2008**, *130*, 10187–10198.

(18) (a) Mitoraj, M. P.; Michalak, A.; Ziegler, T. *J. Chem. Theory Comput.* **2009**, *5*, 962–975. (b) Radon, M. *Theor. Chem. Acc.* **2008**, *120*, 337–339. (c) Michalak, A.; Mitoraj, M.; Ziegler, T. *J. Phys. Chem. A* **2008**, *112*, 1933–1939. (d) Mitoraj, M.; Michalak, A. *J. Mol. Model.* **2007**, *13*, 347–355.